Nuclear Instruments and Methods in Physics Research B 361 (2015) 363–371

Contents lists available at ScienceDirect

Nuclear Instruments and Methods in Physics Research B

journal homepage: www.elsevier.com/locate/nimb

Second generation laser-heated microfurnace for the preparation of microgram-sized graphite samples

Bin Yang, A.M. Smith *, S. Long

Australian Nuclear Science and Technology Organisation, New Illawarra Road, Lucas Heights, NSW 2234, Australia

ARTICLE INFO

Article history:
Received 28 November 2014
Received in revised form 2 February 2015
Accepted 2 February 2015
Available online 19 March 2015

Keywords:
AMS
Accelerator Mass Spectrometry
Graphitisation
Laser furnace
Micro-sample

ABSTRACT

We present construction details and test results for two second-generation laser-heated microfurnaces (LHF-II) used to prepare graphite samples for Accelerator Mass Spectrometry (AMS) at ANSTO. Based on systematic studies aimed at optimising the performance of our prototype laser-heated microfurnace (LHF-I) (Smith et al., 2007 [1]; Smith et al., 2010 [2,3]; Yang et al., 2014 [4]), we have designed the LHF-II to have the following features: (i) it has a small reactor volume of 0.25 mL allowing us to completely graphitise carbon dioxide samples containing as little as 2 μg of C, (ii) it can operate over a large pressure range (0–3 bar) and so has the capacity to graphitise CO_2 samples containing up to 100 μg of C; (iii) it is compact, with three valves integrated into the microfurnace body, (iv) it is compatible with our new miniaturised conventional graphitisation furnaces (MCF), also designed for small samples, and shares a common vacuum system. Early tests have shown that the extraneous carbon added during graphitisation in each LHF-II is of the order of 0.05 μg, assuming 100 pMC activity, similar to that of the prototype unit.

We use a 'budget' fibre packaged array for the diode laser with custom built focusing optics. The use of a new infrared (IR) thermometer with a short focal length has allowed us to decrease the height of the light-proof safety enclosure. These innovations have produced a cheaper and more compact device. As with the LHF-I, feedback control of the catalyst temperature and logging of the reaction parameters is managed by a LabVIEW interface.

Crown Copyright © 2015 Published by Elsevier B.V. All rights reserved.

1. Introduction

At ANSTO, we are equipped with two tandem accelerators: the 2 MV (million volt) STAR and the 10 MV ANTARES machines, both used for radiocarbon measurement. Two new radiocarbon-capable tandem accelerators, a 1 MV and a 6 MV machine, are currently being added to the Centre for Accelerator Science at ANSTO. With the increasing number of AMS machines, we need to increase our graphitisation capability for the preparation of radiocarbon samples.

Since establishment of radiocarbon AMS, many laboratories worldwide have worked to improve their capability for AMS of smaller and smaller carbon samples. Notable amongst the laboratories that prepare and measure 'micro' graphite samples are the KCCAMS Laboratory, with a 2 μg of C capability [5], and the VERA laboratory with a 1 μg of C capability [6]. Some laboratories have bypassed the graphitisation step completely and operate gas (CO_2) ion sources, for instance the ETH laboratory with a 1 μg of C capability [7]. Comparison of the performance of these and other laboratories, for the preparation and measurement of 'micro-carbon' samples, is beyond the scope of this paper.

At ANSTO we have chosen to graphitise our small samples for AMS. Development of the laser-heated microfurnaces LHF-II is one path to improving our throughput of ultra-small radiocarbon samples [1–3]. Based on our operational experience with the prototype laser-heated microfurnace (LHF-I), we designed and manufactured a second generation device, LHF-II, with the aim of producing ~5 μg carbon samples with high reliability and ease. One important application of the LHF-II is for radiocarbon measurement of carbonaceous gases and particles in ice sheets – the ability to reliably prepare and to analyse ultra-small samples is required in such investigations due to the very limited quantity of CO, CO_2 and CH_4 in ice core bubbles and of carbon particulate matter in the ice. Reliability is important for such projects as expedition costs are high. Moreover, there are many other applications at ANSTO that involve small samples for ^{14}C analysis, in fields such as chronology, archaeometry, palynomorphs (pollen, micro-foramifera, phytoliths), diatoms, organic fractions from archaeological material (e.g. mummies, cooking vessels, tool residues), biomedical, DNA (e.g. for brain/neuron cell age) and specific compounds, separated, for example, by preparative gas chromatography.

* Corresponding author.

http://dx.doi.org/10.1016/j.nimb.2015.02.009
0168-583X/Crown Copyright © 2015 Published by Elsevier B.V. All rights reserved.

2. Construction of LHF-II

2.1. Overall system

The LHF-II is designed to produce very small samples with low background and high reproducibility. It is compact, low cost and user friendly. Figs. 1a and 1b show the overall system: the control and display system, the graphitisation reactor, the vacuum system and the cold finger cooling system. The graphitisation reactor is comprised of four parts: (i) the core of the reactor, with three integrated valves for gas and vacuum control, (ii) the laser lens housing, used to focus the IR beam from an optical fibre to ~0.3 mm diameter on the catalyst, (iii) the fibre optic infrared thermometer lens probe, which views the heated target spot, and (iv) the light-proof safety enclosure, including a bottom plate, back plate and a rotatable top box. The IR laser diode module is installed on the back plate inside the enclosure and is connected to the lens housing by an optical fibre. Fig. 1c is an exploded view of the graphitisation reactor.

2.2. Reactor core

The core of LHF-II is machined from a solid block of stainless steel (64 × 64 × 26 mm) and internal surfaces are electro-polished. Viton o-rings are used to seal the valves, miniature pressure transducer and the 3 mm thick, 25 mm diameter quartz window, transparent to IR from the incident laser beam and from black body emission from the heated target. Fig. 2a shows a plan view of the cross section of the core, showing three valves and three ports. The three ports and the cold finger are laser welded to the block. One port is connected to the vacuum/H_2 manifold and another port is connected to the CO_2 sample transfer flask or breakseal cracker. The third port is spare for future development. The valves permit connection to vacuum/H_2 manifold and sample CO_2 and allow the reaction volume to be isolated. Fig. 2b is side view of the central cross section of the core, revealing the reaction volume and the positions of the stainless steel cold finger, crucible and quartz window. The volume of the isolated reactor is 0.25 mL, calculated by measuring the pressure of a known quantity of CO_2 gas in the reactor. The catalyst is placed in a gold-plated quartz crucible (4 mm high, 4 mm diameter, 2.0 mm radius hemispherical recess) directly under the quartz window.

2.3. Vacuum system

Fig. 3 is a photograph of the vacuum manifold assembled on the work bench, also partially shown in Fig. 1a. This manifold has six ports for connection to graphitisation modules. The main vacuum pipe is placed horizontally under the bench and is connected to a turbomolecular pumping station, a MKS Baratron gauge for measuring hydrogen pressure and for calibrating the miniature pressure sensors used in the microfurnaces, a cold cathode gauge

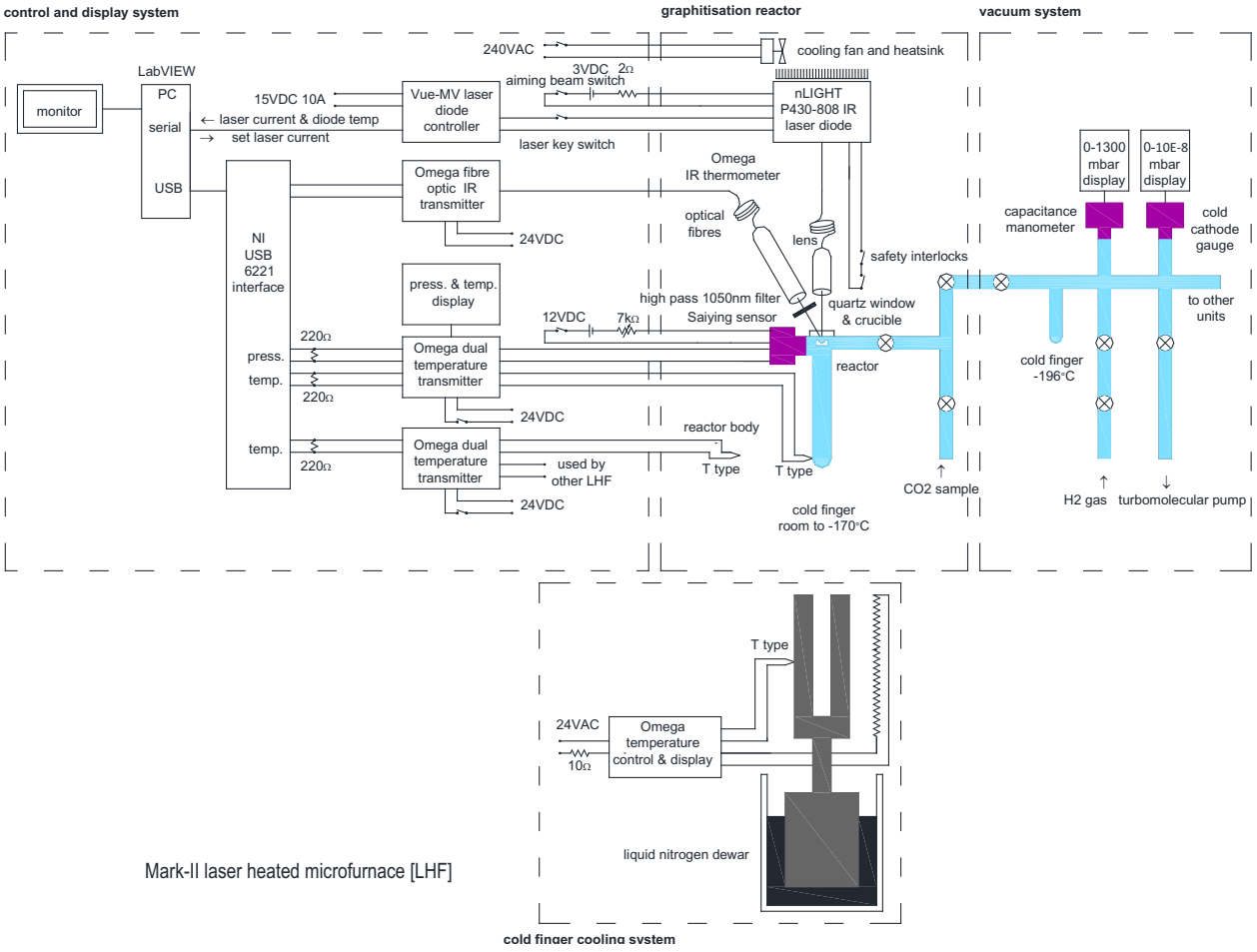

Fig. 1a. Block diagram of one LHF-II: units a and b share the same PC interface, LabVIEW control and vacuum/gas manifold. The National Instruments interface NI USB-6112 accepts 0–4.8 V DC signals, provided by 220 Ω resistors in the 4–22 mA current loop from the Omega temperature transmitters. The miniature Saiying pressure transducer is 0–3 bar.

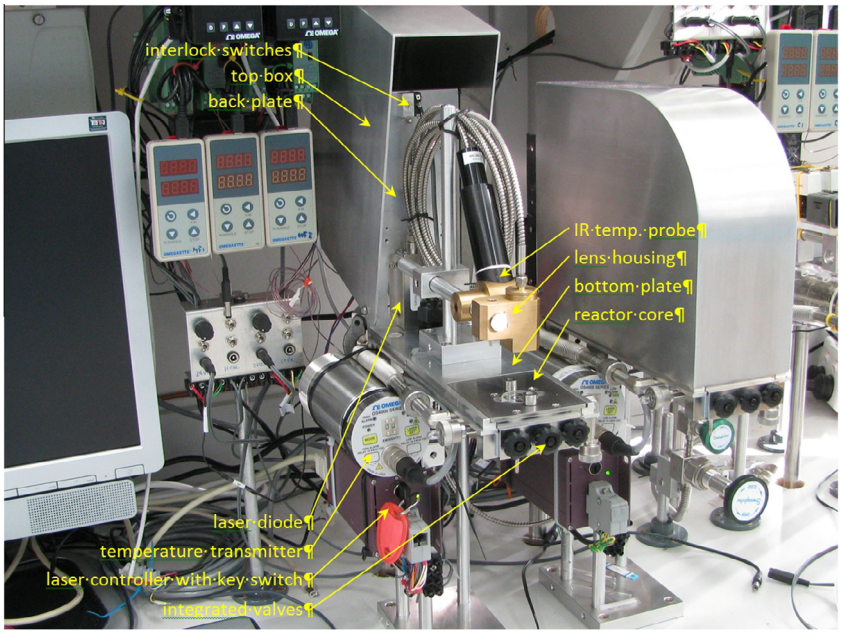

Fig. 1b. Photograph of LHF-IIa (with safety enclosure opened) and LHF-IIb. The components are indicated: stainless steel core with three integrated valves, brass laser focusing lens housing, fibre optic infrared thermometer lens probe with the temperature transmitter, light-proof safety enclosure (including bottom and top plates and rotatable lid), IR laser diode module (attached to the back plate and connected to the lens housing by optical fibre), laser controller with key switch for the laser beam, valve for controlling H_2 gas, computer monitor for LabVIEW control and logging.

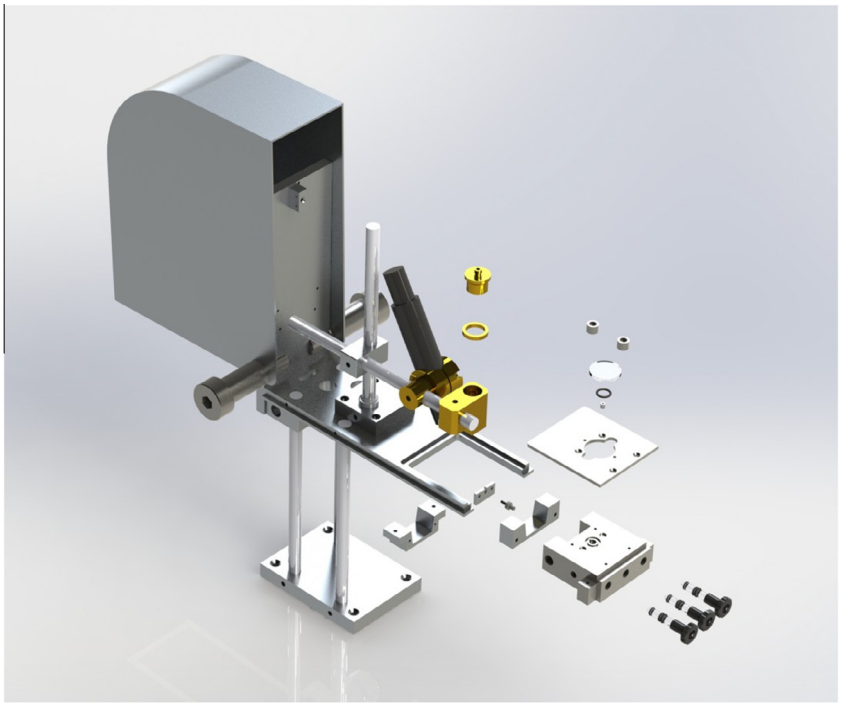

Fig. 1c. Exploded view of LHF-II, showing its modular construction. Standard laboratory scaffolding (MetApp, Australia) is used for the support structure.

for monitoring system vacuum and a cold finger for trapping any residual CO_2 gas and water in the manifold. Seven tubes pass vertically passing through the bench. These tubes are connected to the two laser-heated LHF-II units, to four conventionally heated miniaturised furnaces (MCF) and to a high purity hydrogen source (centre of photograph). Each graphitisation unit is linked to the manifold through a stainless steel bellows and a 90° angle valve.

2.4. Cold finger cooling system

The system for refrigerating the integrated stainless steel cold finger was described in [4]. This operates separately from the LabVIEW control system and permits the cold finger temperature to be rapidly changed between room temperature and −160 °C, with modest use of liquid nitrogen.

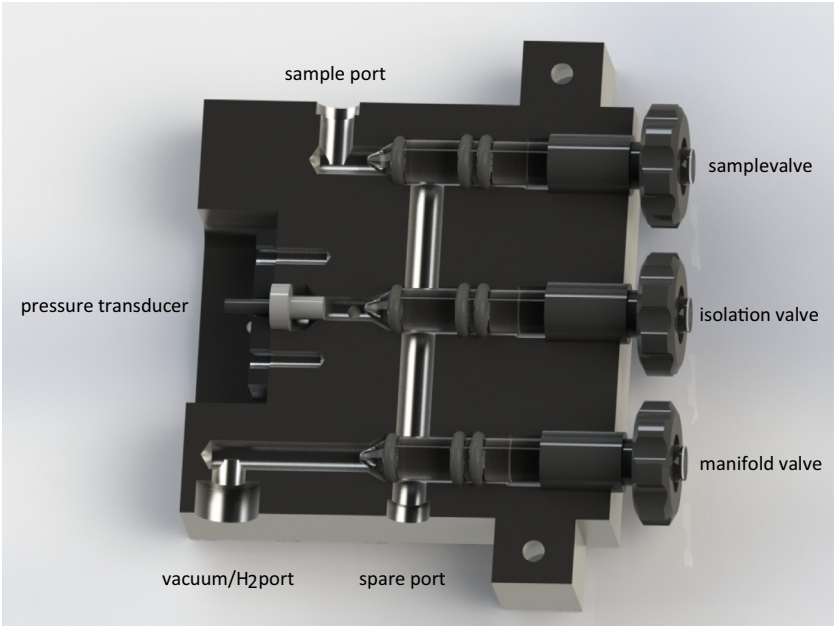

Fig. 2a. Cross section of the core. This is machined from a solid stainless steel block and comprises the gas reactor, three integrated valves and three openings to which ports are laser welded for connect to the gas manifold (vacuum/H_2) the CO_2 sample and a spare (sealed) port.

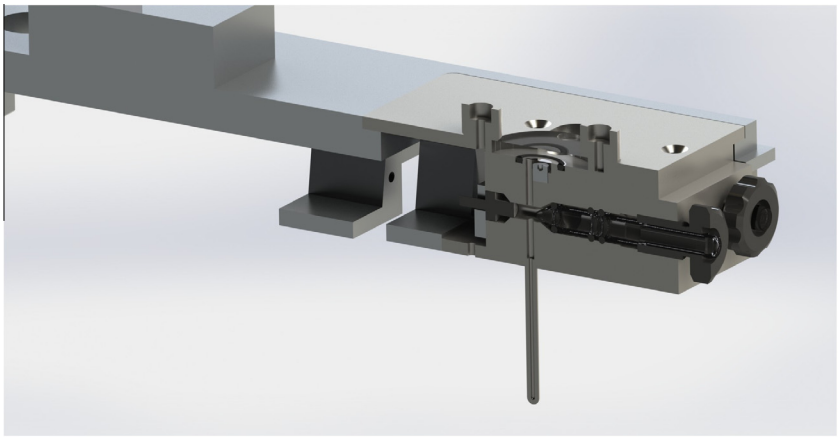

Fig. 2b. Side view of central cross section of the core shows the reactor with the cold finger, 3.5 mm diameter pressure sensor, reactor valve, quartz crucible, quartz window and o-rings.

2.5. Laser system

In LHF-II, a laser diode (nLIGHT, NL-P430-0808) is installed directly on the back plate inside the light-proof safety enclosure and is coupled to the focusing optics by a fibre light guide. Tin foil pressed between the laser diode and the back plate ensures good thermal conductivity for heat transfer. A heat sink provided with a fan is mounted on the outside of the back plate to cool the laser diode during operation. This simple cooling system is sufficient to maintain the laser diode below 30 °C during use with a room temperature of 24 °C, well within its operating specifications. The laser is driven by a compact controller (VueMetrix, Vue-MV-12-01), readily interfaced to the LabVIEW control system. Inside the safety enclosure, laser beam is delivered by a (coiled) 2 m armoured fibre optic cable to the target through a custom built lens housing containing a single lens (f = 20 mm, 16 mm diameter). The laser is also provided with a red aiming beam, a separate visible light source that uses one of the fibres in the fibre bundle. This permits the laser to be precisely positioned and aimed prior to operation, thereby improving safety. The overall laser system is compact and economical, unlike the expensive packaged industrial laser used in the prototype unit. The size of the focused beam is also inherently smaller than the prototype unit due to the different focusing geometry and smaller diameter of optical fibre.

2.6. IR thermometer

The temperature of catalyst is measured with a high speed industrial fibre optic infrared transmitter (OMEGA Engineering Inc, OS4000) with a temperature lens probe (L1-2-3-3) that can measure temperatures from 300 to 1200 °C, using black body IR at 1200–2600 nm. The temperature lens probe has small size (25 mm diameter, 120 mm length), with a focal distance of 50 mm, and is placed behind the laser lens housing at 30° to the vertical. It is also provided with a visible red aiming beam for alignment. Previously, we found that the scattered heating laser beam interferes with temperature measurement. To resolve this problem, a high-pass optical filter is placed on the front of the

Fig. 3. Photograph of the manifold with six ports for connection to graphitisation modules: two LHF and four MCF furnaces. The main vacuum pipe is placed horizontally under the table and it is connected to a turbomolecular pumping station, an MKS Baratron gauge, an active cold cathode gauge and a cold finger for trapping any residual CO_2 gas and water in the manifold.

probe to block any light with wavelength shorter than 1050 nm, including scattered laser light (808 nm), from entering the detector. The output signal (1–5 VDC) of the temperature transmitter is interfaced to the LabVIEW control system. This permits the temperature of the catalyst to be automatically controlled through feedback control of the laser power. This low cost IR thermometer has a smaller size and a much shorter focal distance than that used in the prototype unit, allowing us to fit it within a much smaller light-proof safety enclosure.

2.7. Pressure transducer and thermocouples

To measure the pressure inside the reactor we use a miniature 3.5 mm diameter, 0–3 bar absolute pressure transducer (Saiying Electronic Technology Development Inc., MTC-190). This transducer allows us to perform graphitisations at elevated pressures, increasing the capacity of LHF-II to samples of up to 100 μg of carbon. Unlike other pressure transducers used previously, we have found that this transducer is not adversely affected by the presence of H_2 gas and operates stably over time. It is excited by 8.3 VDC and has an output signal of 5–125 mV. In order to increase the ratio of signal/noise, the output signal is amplified and converted to a 1–4.8 VDC signal by a 'Dual DIN Rail Temperature Transmitter' (OMEGA Engineering Inc., TXDIN70 Series). The converted signal is interfaced to the LabVIEW control system. Additionally, temperature signals from two T-type thermocouples are also converted to 1–4.8 VDC signals by these units so that the reactor body and the cold finger temperatures can be logged.

2.8. Data acquisition and temperature control

LabVIEW (National Instruments, Inc.) software, in conjunction with the NI USB-6221 interface, is used to record experimental parameters during graphitisation and to maintain the catalyst temperature. Fig. 4 shows a control panel in the LabVIEW program. We record the following parameters each second of the reaction: (i) the reactor pressure (Saiying pressure transducer), (ii) the temperature of the cold finger (thermocouple); (iii) temperature of the reactor body (thermocouple), and (iv) the temperature of catalyst (OS4000 transmitter). Communication between the laser controller and the computer is through a USB port. Selected parameters like laser current, laser power and diode temperature are displayed and logged by LabVIEW.

During graphitisation, the pressure in the reactor may drop by up to a factor of ten. It is a challenge to keep the catalyst at a constant temperature (generally 600 °C) under such a large pressure variation where convective losses are changing as the gases CO_2 and H_2 are consumed. The LabVIEW program maintains the temperature of the catalyst at a pre-set value by adjusting the laser current during the reaction. To optimise the temperature control feedback algorithm, we simulated the pressure drop during graphitisation by dropping the pressure of pure H_2 inside the reactor and manually adjusting the laser current to maintain the catalyst at 600 °C. The relation between the current and pressure is shown in Fig. 5. It is a described by the simple equation:

$$I(P) = I_0 + C_1 \times \log(P) \quad (1)$$

where $I(P)$ is the laser current at pressure P and I_0 and C_1 are constants. In addition, we also confirmed that the relationship between laser current and laser power is linear by using a laser power meter [Coherent, FieldMaxII-TO™]. From this and Eq. (1) the laser current is automatically controlled by the following equation:

$$I(P) = I_0 + C_2 \times (T - T_0 + T_{\text{offset}}) \times \log(P) \quad (2)$$

where T_0 is the pre-set temperature, and T_{offset} is a parameter that allows the operator to adjust the temperature manually during graphitisation when necessary. The values of the constants I_0 and C_2 were further refined during later graphitisations of test samples.

2.9. Preparation of catalyst

Good quality catalyst is essential for the graphitisation of micro-samples. Important characteristics include the inherent C and Li content, the reaction speed and efficiency as well as the ability to press the material into targets [3]. Li can be a problem for ^{14}C measurement in the 4+ charge state, as we do on the ANTARES

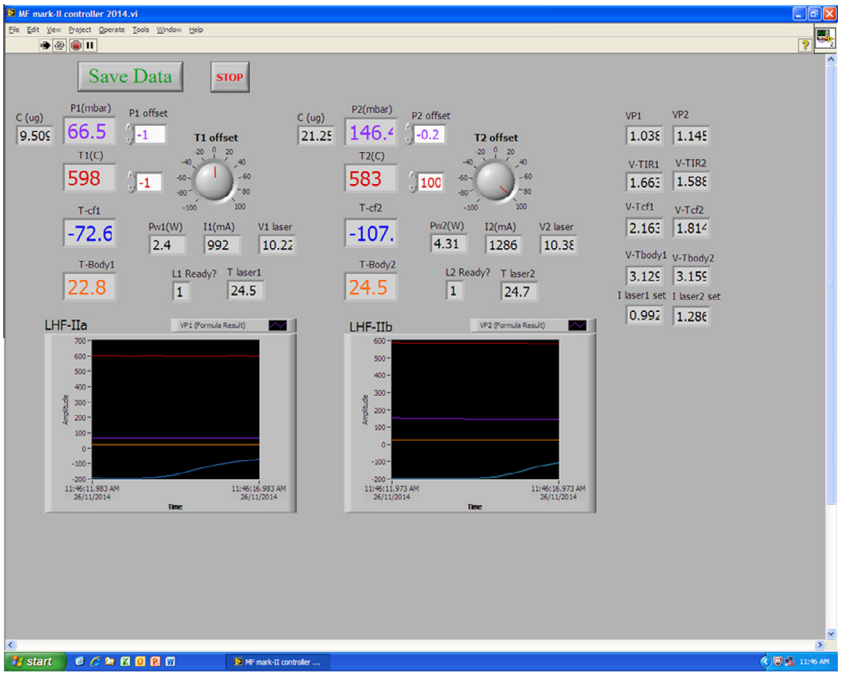

Fig. 4. shows a control panel window in the LabVIEW program.

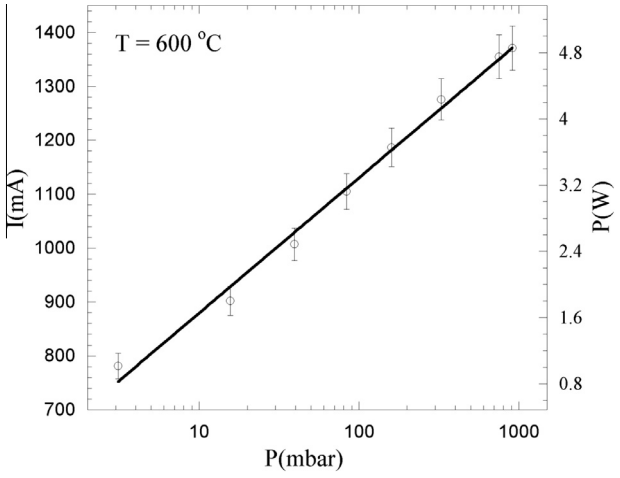

Fig. 5. Current and the corresponding power of the IR laser needed to heat 0.6 mg of iron powder up to 600 °C in H_2, at different pressures. The relationship between the current and the pressure is given by I (mA) = 629 + 251 × log (P mbar), with R = 0.996.

accelerator, since the dimer $^{7}Li_2$ is injected along with ^{14}C and $^{7}Li^{2+}$ passes into the detector along with $^{14}C^{4+}$ which can lead to excessive dead times. After trialing many commercially available materials, we found that the best catalyst is produced by reducing 99.999% Fe_2O_3 powder (Sigma Aldrich, product code 529311) in high purity H_2 gas. This high purity Fe_2O_3 powder has very small particle size and acceptable C and Li content. To begin with, we reduced Fe_2O_3 powder in the quartz crucible within the microfurnace, immediately prior to graphitisation However, two problems appeared: (i) the Fe_2O_3 is vigorously reduced once the laser power is applied and about half could be lost from the crucible, affecting the efficiency of carbon yield and increasing the reaction time; and (ii) the Fe_2O_3 powder that remained inside the crucible was only partially reduced as the laser beam only irradiates part of the powder. This is undesirable, because residual Fe_2O_3 can affect the performance of the sample during AMS due to the presence of oxygen. Furthermore, it appears that Fe_2O_3 can absorb Li from the quartz itself as it is being reduced. For this reason we tried plating the quartz crucibles with a thin layer of gold but this was only partially successful. Hence, it is our practice to separately reduce Fe_2O_3 in large batches and to test its performance in the accelerator prior to use as a catalyst.

For this propose, we produced a dedicated system for Fe_2O_3 reduction. Fig. 6 shows the system comprised of a glass tube, a cold finger and a MKS Baratron gauge. About 140 mg of Fe_2O_3 is loaded into the end of the glass tube with a plug of quartz wool to prevent movement of the powder. The manifold is filled with 800 mbar of H_2; the cold finger is placed in liquid nitrogen to trap H_2O and any evolved CO_2. The end of the tube is heated to 600 °C in a tube furnace and the MKS gauge permits the reaction to be monitored. It takes approximately 5 h to complete the reaction, producing ~100 mg of Fe powder. Preparation of catalyst with very low Li contamination requires selection of glass tubing with very low Li levels or a tube made by from another material such as Al_2O_3.

3. LHF-II performance

3.1. Graphitisation procedure

We apply two-step H_2O trapping during graphitisation, firstly at −70 °C then at −160 °C. This procedure evolved from our earlier study [3] that showed CO_2 is completely reduced to CO within 5 min of applying laser power. Once the CO_2 has been reduced we are able to reduce the cold finger temperature for more efficient trapping of water vapour which improves the reaction speed and efficiency [8]. The entire procedure takes typically one hour to prepare a sample following these steps:

(1) Open the safety housing and remove the quartz window; Weigh and load 0.6 mg of Fe catalyst into a quartz crucible and place it in the centre of the reactor.

Fig. 6. Shows the manifold for reducing iron oxide that contains a glass tube, a cold finger and MKS Baratron gauge.

(2) Replace the quartz window and close the safety housing. Connect the CO_2 sample transfer flask to the microfurnace. Turn on the vacuum pump and open all three reactor core valves to evacuate the microfurnace.
(3) When the vacuum has reached 1.5×10^{-4} mbar, set the cold finger temperature to −160 °C, close the manifold valve then open the valve on the sample transfer flask for 60 s to transfer the CO_2 sample into the microfurnace reactor cold finger.
(4) Close the isolation and sample valves then open the manifold valve. Set the cold finger temperature to −70 °C and record the pressure of the CO_2 in the reactor (P_{CO_2}).
(5) Set cold finger temperature to −160 °C. Open the isolation valve and H_2 valve slowly, allowing H_2 to fill the reactor to a pressure ~2.5 times of P_{CO_2}.
(6) Close the isolation valve and set cold finger temperature to −70 °C and record the pressure of the CO_2 and H_2 in the reactor ($P_{CO_2+H_2}$). Turn on the laser beam with the key switch to initiate graphitisation.
(7) After 5 min or so, when the pressure has dropped to ~1/2 of $P_{CO_2+H_2}$, set the cold finger temperature to −160 °C.
(8) After about 30 min of graphitisation, turn off the laser beam with the key switch, stopping graphitisation.
(9) Set cold finger temperature to −70 °C and record the pressure of the reactor as P_{end}. Calculate the efficiency of carbon yield as explained below.
(10) Press the graphite and catalyst into a 1 mm diameter rear-loaded target for AMS.

Recent tests have shown that no measurable CO_2 remains behind after this two-step H_2O trapping procedure. Analysis of the residual gas following a similar procedure in LHF-I using quadrupole mass spectrometry showed that CO and CH_4 were absent [4]. Fig. 7 shows the experimental parameters recorded by LabVIEW for the graphitisation of a 5 μg carbon sample as a function of time, following the above procedure. The small drop in pressure at 21 min when the CF was decreased to −160 °C and the small rise at 30 min when the CF was increased to −70 °C are a consequence of changing the mean temperature of the gas; had CO_2 been present a much larger change would have been observed. Fig. 8 is a photograph of the catalyst in a crucible following graphitisation of 30 μg of carbon. There is a visible ring of graphite deposited around the ~0.3 mm diameter focused laser beam. We have varied the focused spot size but found that the graphitisation time remains fairly constant. We prefer to use a tightly focused beam because lower laser power is required for graphitisation and the crucible and surrounds stay cooler. This significantly decreases the addition of Li to the sample and probably also extraneous carbon.

3.2. Efficiency of carbon yield

The reaction efficiency is calculated on the assumption that residual gas following graphitisation with the cold finger at −70 °C contains only H_2 and CO and no CO_2, CH_4 or H_2O. Under these conditions,

$$\text{Efficiency} = 0.5 \times (P_{CO_2+H_2} - P_{CO_2} - P_{end})/P_{CO_2} \quad (3)$$

If, however, the Fe_2O_3 had not been completely reduced to Fe before graphitization this will take place in the furnace, consuming some H_2. This causes a pressure decrease $P_{Fe_2O_3}$. In a separate

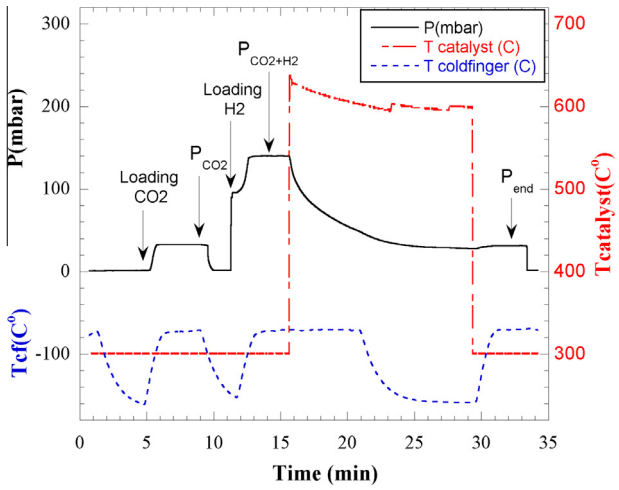

Fig. 7. Shows the experimental parameters recorded during the graphitisation of 5 μg of carbon sample as a function of time.

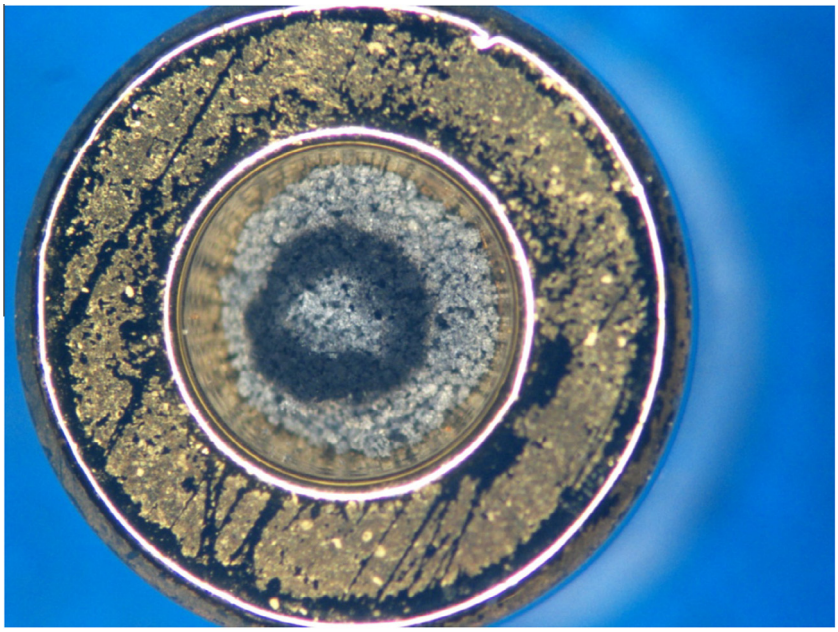

Fig. 8. Shows a photograph of the catalyst in the crucible after the graphitisation of 30 μg of carbon. There is visible ring of graphite deposited around the focused laser beam. The diameter of the crucible is 4 mm and of the hemispherical recess is 2 mm.

experiment, $P_{Fe_2O_3}$ was measured by the complete reduction of 0.6 mg of pre-prepared Fe catalyst in the microfurnace. By also taking $P_{Fe_2O_3}$ into account, the efficiency is then:

$$\text{Efficiency} = 0.5 \times (P_{CO_2+H_2} - P_{CO_2} - P_{end} - P_{Fe_2O_3})/P_{CO_2} \quad (4)$$

Fig. 9 shows the efficiency calculated by Eq. (4) with $P_{Fe_2O_3}$ = 20 mbar for a set of samples of varying carbon masses down to 2 μg. As can be seen, some of the calculated efficiencies exceed 100% for some of the smaller samples. This is presumably due to differing degrees of reduction for the Fe_2O_3 catalyst. The errors are larger for the smaller samples due to errors in the pressure measurement.

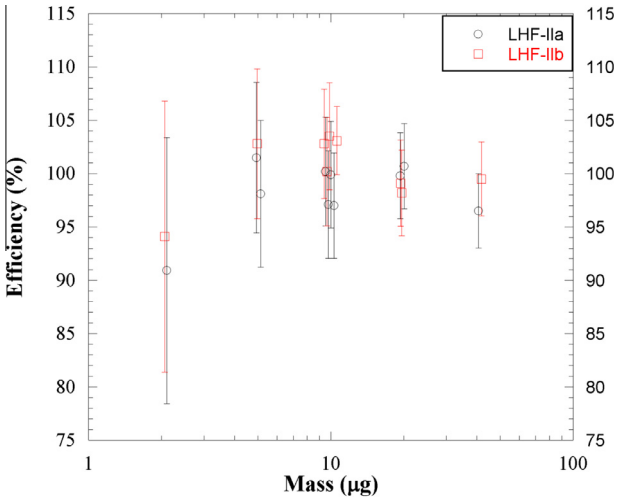

Fig. 9. Shows the efficiency calculated by Eq. (4) and $P_{Fe_2O_3}$ = 20 mbar for a set of samples of varying carbon masses down to 2 μg. Within errors, they are all close to 100%.

4. AMS performance

4.1. C13 current/C mass

Radiocarbon targets containing 5–20 μg of C graphitised with reduced Fe_2O_3 in the LHF-IIa,b produce ~13 nA of $^{13}C^{4+}$ for each μg of C in the HVE 846B ion source on the ANTARES accelerator. Under normal measurement conditions ~48% transmission for ^{12}C in the 4+ charge state is achieved. 5 μg samples produce a useable current for ~30 min, with larger samples lasting longer. Because of the ring-shaped deposition of graphite on the catalyst, the carbon can be 'buried' under the non-C bearing catalyst on loading the AMS targets. This can result in a delay of 5 min or so before the extracted C beam reaches full intensity as the Fe is sputtered away. It is our intention to decrease the diameter of the sample recess from the present 1.0 mm to 0.5 mm, with a consequent decrease in the amount of catalyst from the present ~0.6 mg of Fe, so lessening this effect.

4.2. Extraneous carbon

'Extraneous carbon' is contaminant carbon that is added to the sample carbon during processing. This may have a number of sources [9] and the amount and ^{14}C activity of this material must be determined in order to apply a correction to an AMS measurement. For such corrections to be valid it is important to keep to routine procedures during sample handling, graphitisation and target loading so that the mass and activity of the extraneous carbon remains as constant as possible.

The simplest method to quantify the extraneous carbon is to assume that this material has an activity of 100 pMC and to prepare a series of differently-sized ^{14}C depleted 'blanks'. We then expect the measured activity to scale linearly with the inverse of mass [10] and [references therein]. Fig. 10 shows the result of such an experiment for the two LHF-II a and b, where linear regression was used to fit a line to the points using $1/(\text{pMC error})^2$ as the weighting factor. In this case we used reduced Fe_2O_3 as the catalyst and 0.03 ± 0.01 pMC CO_2 and measured the samples on ANTARES. The results are consistent with 0.043 ± 0.010 μg and 0.047 ± 0.008 μg of extraneous (assumed) 100 pMC carbon for each furnace. This is very similar to that found for the prototype LHF [2].

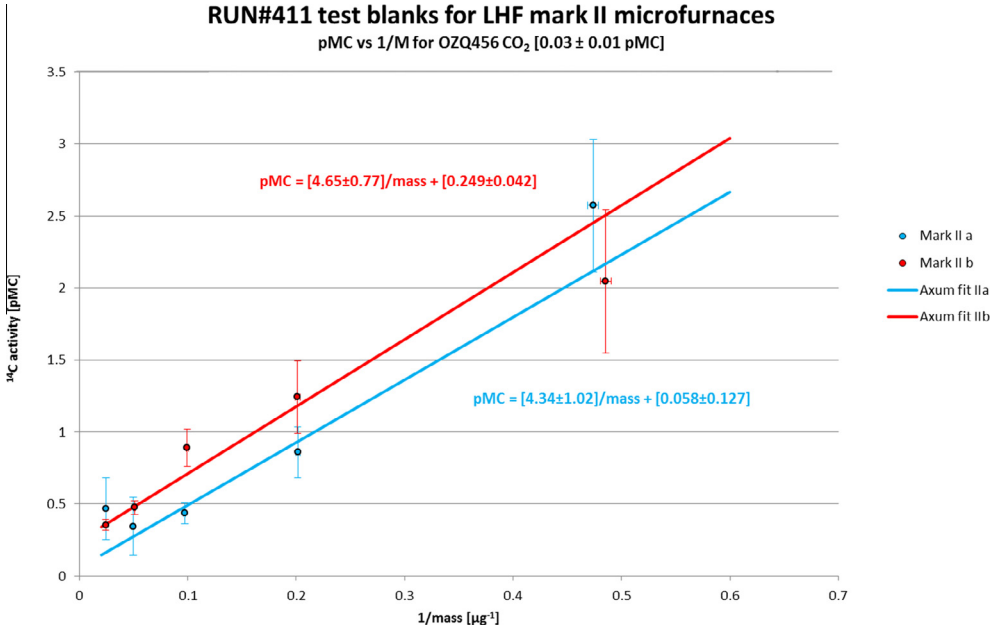

Fig. 10. Determination of extraneous carbon added during graphitisation by using ^{14}C-depleted CO_2 samples of varying mass m and plotting the measured activity versus 1/m. The fitted lines and equations were generated by weighting the dependent variable pMC by 1/(pMC error)^2.

A more thorough analysis to determine the actual activity as well as the mass of extraneous carbon requires the preparation of differently sized samples of ^{14}C depleted as well as an active material. The procedure is explained in [10]. This is a time consuming process and ideally should be repeated each time any experimental conditions or apparatus are changed. We will undertake such an analysis for the two LHF-II using reduced Fe_2O_3, the depleted CO_2 mentioned above and 87.42 ± 0.24 pMC CO_2 obtained from a commercial cylinder. Use of CO_2 obtained from cylinders is preferred as this bypasses uncertainties about extraneous carbon added through other processing techniques such as combustion of hydrolysis.

5. Conclusion

We estimate that the volume of each LHF-II reactor is about 0.25 mL, about half that of the LHF-I. The LHF-I can graphitize CO_2 gas containing 5 μg samples with a carbon yield over 90%, and we have shown that the LHF-II is capable of graphitising 2–3 μg samples with a carbon yield of over 90% and with a yield approaching 100% for larger samples. Use of a 0–3 bar pressure transducer has allowed extension of sample masses towards 100 μg of C. The amount of extraneous carbon added during graphitisation is of the order of 0.05 μg of 100pMC, similar to that found for LHF-I. To date 49 samples have been prepared in LHF-IIa and 34 in LHF-IIb, spanning 2–85 μg of C, with no sample failures and efficiencies all near 100%. We have not observed any 'memory' in the LHF-II, nor in LHF-I.

These second generation laser-heated furnaces are of compact size, for both the graphitisation reactor and the ancillary systems. They are more affordable than the prototype unit because the laser system has been assembled from discrete units, rather than purchasing an entire commercial system. Furthermore, many of the other components are commercial available at reasonable prices.

Future work will be directed towards measurement of the actual activity and mass of extraneous carbon added during the graphitisation process and reactor memory tests. We continue to trial new catalysts with a view to finding superior material. We aim to decrease the diameter of the sample recess from the present 1.0–0.5 mm, with a consequent decrease in the amount of catalyst required. We also intend to modify the three valves in the LHF-II and the MCF reactor cores to operate with solenoids, permitting future automation of the procedure.

References

[1] A.M. Smith, Q. Hua, V.A. Levchenko, New developments in micro-sample ^{14}C AMS at ANSTO, INQUA 2007 abstracts, Quatern. Int. 167–168 (2007) 390.
[2] A.M. Smith, Q. Hua, A. Williams, V. Levchenko, Bin Yang, Developments in micro-sample ^{14}C AMS at the ANTARES AMS facility, Nucl. Instr. Methods Phys. Res. B 268 (2010) 919–923.
[3] A.M. Smith, Bin Yang, Quan Hua, Michael Mann, Laser-heated microfurnace – gas analysis & graphite morphology, Radiocarbon 52 (2–3) (2010) 769–782.
[4] Bin Yang, A.M. Smith, Quan Hua, A cold finger cooling system for the efficient graphitisation of microgram-sized carbon samples, Nucl. Instr. Methods Phys. Res. B 294 (2013) 262–265.
[5] G.M. Santos, J.R. Southon, S. Griffin, S.R. Beaupre, E.R.M. Druffel, Ultra small-mass AMS 14C sample preparation and analyses at KCCAMS/UCI facility, Nucl. Instr. Methods Phys. Res. B 259 (2007) 293–302.
[6] J. Liebl, P. Steier, R. Golser, W. Kutschera, K. Mair, A. Priller, I. Vonderhaid, E.M. Wild, Carbon background and ionization yield of an AMS system during ^{14}C measurements of microgram-size graphite samples, Nucl. Instr. Methods Phys. Res. B 294 (2013) 335–339.
[7] S.M. Fahrni, L. Wacker, H.A. Synal, S. Szidat, Improving a gas ion source for ^{14}C AMS, Nucl. Instr. Methods Phys. Res. B 294 (2013) 320–327.
[8] A.M. Smith, Vasilii V. Petrenko, Quan Hua, John Southon, Gordon Brailsford, The effect of N_2O on the graphitization of small CO_2 samples, Radiocarbon 49 (2) (2007) 245–254.
[9] J. Southon, Graphite reactor memory – where is it from and how to minimize it?, Nucl Instr. Methods Phys. Res. B 259 (1) (2007) 288–292.
[10] Q. Hua, U. Zoppi, A.A. Williams, A.M. Smith, Small-mass AMS radiocarbon analysis at ANTARES, Nucl. Instr. Methods Phys. Res. B 223–224 (2004) 284–292.